Title

Active cancellation – A means to zero dead-time pulse EPR

Authors

Franck, John M
Barnes, Ryan P
Keller, Timothy J
et al.

Publication Date

2015-12-01

DOI

10.1016/j.jmr.2015.07.005

Peer reviewed

HHS Public Access

Author manuscript

J Magn Reson. Author manuscript; available in PMC 2016 December 01.

Published in final edited form as:

J Magn Reson. 2015 December ; 261: 199–204. doi:10.1016/j.jmr.2015.07.005.

Active Cancellation – A Means to Zero Dead-Time Pulse EPR

John M. Franck[#], **Ryan P. Barnes**[#], **Timothy J. Keller**, **Thomas Kaufmann**, and **Songi Han**[2]

Department of Chemistry and Biochemistry, University of California, Santa Barbara, California 93106

[#] These authors contributed equally to this work.

Abstract

The necessary resonator employed in pulse electron paramagnetic resonance (EPR) rings after the excitation pulse and creates a finite detector dead-time that ultimately prevents the detection of signal from fast relaxing spin systems, hindering the application of pulse EPR to room temperature measurements of interesting chemical or biological systems. We employ a recently available high bandwidth arbitrary waveform generator (AWG) to produce a cancellation pulse that precisely destructively interferes with the resonant cavity ring-down. We find that we can faithfully detect EPR signal at all times immediately after, as well as during, the excitation pulse. This is a proof of concept study showcasing the capability of AWG pulses to precisely cancel out the resonator ring-down, and allow for the detection of EPR signal during the pulse itself, as well as the dead-time of the resonator. However, the applicability of this approach to conventional EPR experiments is not immediate, as it hinges on either (1) the availability of low-noise microwave sources and amplifiers to produce the necessary power for pulse EPR experiment or (2) the availability of very high conversion factor micro coil resonators that allow for pulse EPR experiments at modest microwave power.

Graphical Abstract

[2] Corresponding Author: songi@chem.ucsb.edu.

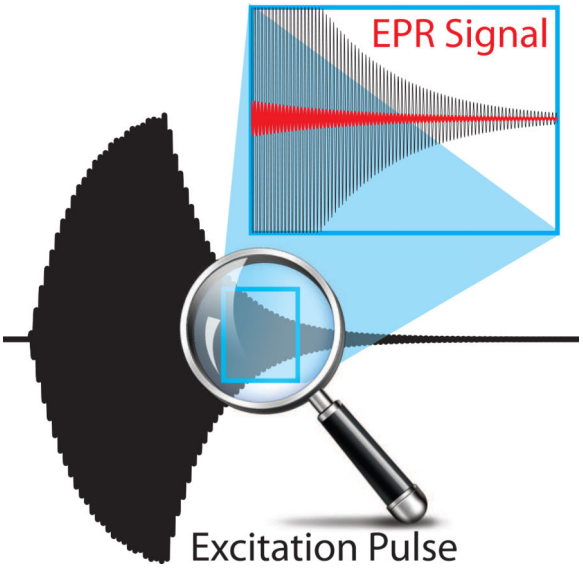

Keywords

Pulse EPR; Arbitrary Waveform Generation; Active Cancellation; AWG EPR; dead-time limited EPR; FPGA EPR

Introduction

In recent years pulse electron paramagnetic resonance (EPR) has seen many advances in its ability to study paramagnetic or spin labeled chemical and biological systems of interest due to substantial improvements in instrumentation and measurement methods[1–7] and the necessary theory for quantitative interpretation of data[8–11]. However in the most common applications of pulse EPR at 10 – 35 GHz frequency, the necessary high power microwave pulse, required to excite the magnetic resonance of the electron spin system, induces a ring-down during which the pulse energy dissipates from the resonant microwave cavity. The cavity ring-down causes a finite detector dead time after the microwave pulse that can last up to 20 ns at cavity quality factors common for pulsed EPR measurements, preventing the detection of EPR signals that rapidly decay during this time. This not only limits the prospects for Fourier transform pulse EPR but, more immediately, prevents the detection of fast decaying signals of interest, such as the T_2 of spin labeled proteins in solution state used for evaluating protein dynamics[3,12]. Many have explored ideas to suppress the resonator ringing in magnetic resonance studies; by means of damped circuit designs[13–15], use of orthogonal excitation and detection coils[16–19], by induction mode detection[20], or by use of a suppression pulse to de-charge the resonant circuit from the excitation pulse[21,22]. One of the most common solutions to ring-down at X-band frequencies is to decrease the effective Q-factor of the microwave resonant cavity (*eg.*, by over-coupling) to minimize the ring-down, to as little as 10–200 ns in the best case scenario[23,24], however reduction of the Q-factor also significantly decreases the B_1 conversion factor so one must use very high rf pulse power (~1 kW) to generate sufficient B_1 field strength and compensate for the loss.

Even so, a dead-time of 10-200 ns is too long to fully capture the timescales and signatures of rapidly decaying signal of many electron spin systems of interest.

Expanding on previous ideas[25,26] we completely remove the resonator ring-down and detect signal at all times during or after a pulse by means of a previously unavailable high bandwidth Arbitrary Waveform Generator (AWG) that synthesizes a separate “cancellation pulse”. We capitalize on the fact that the resonator ring-down depends only on the electronic properties of the resonator. Therefore, once the ring-down is accurately measured for given experimental conditions, a modern AWG can faithfully produce a cancellation pulse to precisely and destructively interfere with this ring down, thus unveiling the initially buried EPR signal. We refer to this procedure as “active cancellation” of the resonator ring-down.

Experimental

The accurate cancellation of the resonator ring-down immediately following, and even during the microwave excitation pulse, is enabled by a home-built pulse EPR instrument that features AWG capabilities at 1 GHz bandwidth and 14-bit dynamic range[27], similar to recent developments by others[1,21,28–31]. To realize the full capabilities of the field programmable gate array (FPGA) core of the AWG, originally produced by Bialczak and Martinis et al.[32], we developed a pulse EPR instrument that is entirely coordinated and synchronized by the FPGA[27]. The benefit of centralizing the complete EPR instrument on the FPGA core is the overwhelming simplification of the instrument operation[31,33], a fully phase-locked instrument, and the capability for precise calibration of microwave amplitude, phase, and timing, included as an intrinsic feature of the spectrometer. In fact achieving precise destructive interference of the complex resonator ring-down at the detector is only possible with a phase-locked AWG, microwave source, and detection oscilloscope.

To calculate a cancellation pulse we determine the shape and phase of the excitation pulse's ring-down with the magnetic field set off resonance to prevent the unwanted detection of induced electron spin signal. Precise destructive interference at the signal detector will occur if the shape and phase of the cancellation pulse are achieved at the signal detector. We account for the distortions that occur to the cancellation pulse en-route to the signal detector by applying a transfer-function—this allows us to calculate the necessary pulse shape to be synthesized to achieve the desired cancellation pulse shape at the signal detector, with more precise details given in the SI (Fig SI-1).

In order to detect true EPR signal at any time during or after the excitation pulse, the AWG-generated cancellation pulse must reach the detector without perturbing the spin system dynamics during the time in which we record signal. We avoid the need for two separate pulse sources – one for the excitation pulse, and one for the cancellation pulse that destructively interferes with the resonator ring-down – by implementing a waveguide assembly (Fig 1-A) that splits a given microwave pulse in two, sending one half of the microwave pulse directly to the detector (Fig 1-B “shortcut pathway”) and the other half of the pulse through a delay line leading to the microwave resonator and finally to the detector (Fig 1-B “resonator pathway”). Ultimately both waveforms show up at the detector; the leading of the two waveforms coming from the shortcut pathway and the trailing coming

from the resonator pathway, (Fig 1-B “waveform at detector”). Here the leading edge of the waveform from the resonator pathway is delayed relative to the waveform from the shortcut pathway by approximately 35 ns, due to the length of the delay line (roughly 1.1 m) inserted before the microwave resonator. This 35 ns delay between the waveforms, shown in Fig 1-B and 1-C as vertical red dashed lines, from the two separate pathways “buys” a 35 ns window of time to cancel the excitation pulse's ring down and detect signal, after which time the cancellation pulse enters the resonator and perturbs the spin response to the excitation pulse. We place a 35 ns long cancellation pulse behind the excitation pulse after a set delay (Fig 1-C “synthesized waveform”). The cancellation pulse is designed to destructively interfere with the specific portion of the resonator ring-down that overlaps with the cancellation pulse at the signal detector. We calculate the cancellation pulse by detecting the resonator ring-down, picking a section of the ring-down to cancel (Fig 1-B “waveform at detector” blue dashed line), and taking the negative of that section of the ring-down to form the cancellation pulse (Fig 1-C “synthesized waveform” circled in red). Upon synthesizing the waveform in Fig 1-C, the cancellation pulse follows the excitation pulse, and passes through both the resonator and shortcut pathways (the cancellation pulse is circled in red in both pathways in Fig 1-C). The timing and sequence of the waveforms are designed such that after passing through both the resonator and shortcut pathways, the cancellation pulse from the shortcut pathway precisely overlaps with and destructively interferes with the select section of the resonator ring-down at the detector, resulting in the “cancellation window” highlighted by the vertical red dashed lines in Fig 1-C “waveform at detector”. The cumulative effect of the cancellation pulse from each pathway is shown in the respective colors in Fig 1-C “waveform at detector”. Once the cancellation window is achieved, it is possible to detect electron spin resonance signal from the interaction between the excitation pulse and the spins of the sample alone within the cancellation window. After the 35 ns long cancellation window, defined by the length of the delay line, the cancellation pulse enters the resonator and perturbs the spin response from the excitation pulse (Fig 1-C “resonator pathway” highlighted in the red circle). We discard the last 5 ns of the signal detected inside of the cancellation window to prevent any erroneous signal due to the cancellation pulse.

The current implementation of the delay line and cancellation window is strictly to demonstrate the effectiveness of active cancellation of EPR resonator ring down with AWG capabilities using currently available hardware at hand. In reality, the 35 ns long cancellation window, in which we detect signal, presents a severe limitation to the method as this dramatically extends the experiment to prohibitively long times. One work-around is to increase the length of the delay line, thus increasing the length of the cancellation window. However a simpler solution includes a separate AWG source aimed directly at the signal detector. In this scheme the cancellation pulse only travels to the signal detector, and not the spin-system, allowing one to design the cancellation pulse to destructively interfere with the entirety of the ring-down, such that the entirety of signal could be captured in on shot. Thus, once the high fidelity of AWG pulses for active cancelation can be demonstrated and the merit of the general approach found, alternative and more sustainable hardware solutions will be developed.

Due to the relatively high power of the excitation pulse's resonator reflection, up to 10 W, we implement a two-stage optimization procedure to initially calculate a cancellation pulse

and further optimize the cancellation pulse such that the EPR signal is uncovered and detectable within the cancellation window. In the first stage we attenuate the excitation pulse's high-power ring down to approximately 1 mW and detect the attenuated excitation pulse resonator reflection on a sampling oscilloscope (Tektronix 11801C) (Fig 2-B). We select a 35 ns long portion of the ring-down to cancel and take the cancellation pulse as the negative of this portion of the ring-down (Fig 2-C). We apply the transfer-function to the cancellation pulse in order to preemptively account for the systematic distortions that occur to the cancellation pulse in the shortcut pathway en route to the detector. We place the transfer-function corrected cancellation pulse in the original digital excitation waveform (Fig 2-D) and synthesize the new waveform. Timing is crucial, so that the cancellation pulse is placed at a precisely tuned time after the excitation pulse in series, such that when the cancellation pulse exits the shortcut pathway it is properly aligned with the (delayed) portion of the excitation pulse's resonator ring down that the cancellation pulse was designed to destroy. The fidelity of the cancellation pulse is evaluated by capturing the residual microwave waveform remaining inside of the cancellation window (Fig 2-E). If the power of the residual microwave waveform inside of the cancellation window is above a 2.5 μW threshold (saturation limit of the signal detector) we improve the cancellation pulse shape using the residual waveform in (Fig 2-E) to calculate a new cancellation pulse. We then apply the transfer-function to the new cancellation pulse and add the transfer-function corrected cancellation pulse to the previous cancellation pulse. We iterate this process of additively improving the cancellation pulse until the residual microwave waveform inside of the cancellation window is below 2.5 μW (usually 2-3 iterations). At this point, we proceed to the second stage where we detect the residual microwave waveform inside of the cancellation window with the heterodyne detection train of the spectrometer configured to detect the low power EPR signal on a storage oscilloscope (Agilent MSO7104B). By detecting the un-attenuated residual microwave waveform in the cancellation window, we are able to increase the dynamic range for the amplitude resolution, and with such refinement are able to further reduce the residual microwave waveform to ~ 10 nW (the noise floor of the solid-state amplifier) after employing the same additive cancellation scheme described in stage 1. After these refinement steps, we are able to linearly detect the EPR signal within the cancellation window after background subtraction.

The model system of choice to demonstrate the active cancellation scheme is BDPA (α,γ-Bisdiphenylene-β-phenylallyl) embedded in a polystyrene matrix (45 mmol BDPA/kg PS referred to as BDPA / PS) that presents relaxation times of T_2 ~ 300 ns and T_1 ~ 5 μs[27,34]. To demonstrate the fidelity of the active cancellation method, a near-critically-coupled (Q ~ 900) Bruker MD5 probe head was used to cause a long detector dead-time of 500-600 ns and a B_1 field of approximately 6 MHz at 10 W of pulse power. A 20 W solid-state amplifier array was employed (4 Advanced Microwave PA2803-24 amplifiers arranged in parallel[35]). Due to the power splitting resulting from the delay line assembly, 10 W pulses are achieved in both the shortcut pathway and the delay line / resonator pathway.

Results and Discussion

The two-stage optimization procedure reduces the excitation pulse's cavity reflection from at most 10 W to < 10 nW (noise level of the 20 W pulse amplifier), which amounts to ~ 90 dB

attenuation in total. In an effort to demonstrate that the active cancellation method can be employed as a practical scheme to recover unperturbed EPR signal in the presence of high power microwaves, we detect the Rabi oscillation of the spin system at room temperature during a 400 ns long hard pulse that generates excitation as well as four subsequent inversions of the spin system (Fig 3-A).

To detect signal during the pulse itself using the active cancellation method (signal persists for ~ 500 ns), it is necessary to compile the signal detected in individual cancellation windows (35 ns long) which overlap in time on the trailing edge by 5 ns and span the entire 500 ns time range to capture the signal. Recall the need to detect signal in the 35 ns long cancellation window to ensure the signal detected is due to the influence of the excitation pulse alone, and not by the tandem cancellation pulse interacting with the spins. The EPR signal is detected in each cancellation window by off-resonance background subtraction. By stitching the signal detected from each cancellation window together, we were able to recover the Rabi oscillation of the spins during, as well as after the 400 ns long excitation pulse of the BDPA/PS sample (Fig 3). We observe that the Rabi oscillation precesses about the axis of excitation with a B_1 field strength of approximately *5 MHz* (with 90°, 180°, and 270° times of 50, 95, and 140 ns respectively).

For comparison, the Rabi oscillation of the spin system was also measured via Hahn echoes positioned *after* the decay of the ring-down, where the integrated amplitude of each echo is recorded as a function of increasing length of both the 90° and the 180° pulses (Fig 3). We observe 90°, 180°, and 270° times of 45, 85, and 125 ns respectively, yielding a B_1 field strength of approximately *6 MHz*. When comparing the two methods of measuring the Rabi oscillations, an initial lag period in the nutation frequency is observed in the active cancellation-detected Rabi oscillation, noted in the slightly longer 90° and 180° times. This difference is due to the finite build up time for the excitation pulse's B1 field to reach full amplitude. By comparing the spacing of the 180° and 270° times to the 90° time during the pulse in the active cancellation method, we see this build up time to be ~15 ns. Once the B1 field of the pulse inside of the cavity has built up to maximum strength, the spins then nutate at the expected frequency of *6 MHz* for the given cavity conditions and pulse power.

The key motivation for uncovering the hidden signal under the cavity ring-down, 10 - 200 ns long (depending on the size and dielectric constant of the sample and given resonator conditions) under typical pulsed EPR operations, is to access spin systems with prohibitively short relaxation times. While the measurement of fast decaying T_2 spin systems is not currently possible with our low power implementation we seek to demonstrate that our active cancellation strategy can faithfully uncover signal hidden in the ring-down. We perform T_2 measurements of our model BDPA/PS spin system at room temperature with a previously determined T_2 of 315 ns [27] and with the cavity Q set purposefully to 800, i.e. impractically high for pulsed EPR experiments, to demonstrate the ability of the active cancellation method to recover echoes that are entirely buried in the resonator ring-down with high fidelity. The echo, for a given pulse spacing τ, is recovered in a manner similar to which the Rabi oscillation signal was recovered, that is, the entire echo signal (400 ns long) is recorded piecewise in a series of 35 ns long windows (constrained by the length of the cancellation window) that span the ~ 400 ns long time domain echo signal. Representative

echo traces are shown in the inset of Fig 4. To eliminate any deleterious effects from the FID after the 180° pulse, we implement a two-step, 90_x-τ-180_x and 90_x-τ-180_{-x}, phase cycling scheme, where the inverted phase of the 180 pulse causes the subtraction of the FID when adding the echo signals. The integrated amplitude of each phase-cycle corrected echo is recorded as a function of the inter-pulse spacing τ to generate the T_2 decay curve shown in Fig 4. We observe; echoes that begin to refocus during the end of the 180° pulse (Fig 4-A), echoes during the ring-down (Fig 4-B), and echoes detected after the ring-down has decayed below the saturation limit of the signal detector (Fig 4-C). The time-domain decay of the echoes from sections B and C of Fig 4 fit to a mono exponential decay with a time constant of 314 ± 6 ns, which agrees with the previously determined T_2 of 315 ns for this sample [27]. The distorted echo signal at an inter-pulse spacing of less than 200 ns (Fig 4-A) is likely due to the interference with residual pulse power inside of the resonator, as discussed in the SI.

Conclusion and Outlook

In summary, we find that by actively cancelling the resonator ring-down we can measure unperturbed signal from the EPR spin system at any time during a given pulse sequence, including within the pulse duration and during the pulse ring-down. At the current stage of hardware development, the active cancellation technique is successful with a solid-state amplifier at relatively low power (10-20 W) compared to a TWTA that offers high powers in the 1 kW range as employed for traditional pulse EPR applications. However, with recent advances in resonator design, in particular micro coil resonators with very high conversion factors, it is feasible to carry out many conventional pulse EPR experiments with high fidelity even with low microwave power (W to mW) [23,36–39]. One could thus imagine employing the AC method in conjunction with a micro coil setup in practical pulse EPR settings. Obviously, the utility of the active cancellation method would be more immediate and far greater if traditional TWTAs yielding kW powers can be employed, or if solid-state amplifiers with >100 W output became broadly available.

We see two obstacles to overcome in employing the active cancellation method with the TWTA: (1) the physical limitation of the gated noise from the TWTA saturating the detection electronics and preventing signal detection, which imposes an intrinsic limitation on the microwave power one can apply to the method, and (2) the cancellation waveform fidelity operating in the non-linear output regime of the TWTA. For the active cancellation method to succeed, it is necessary to detect signal while the amplifier is on. Thus, the limitation on the maximum power that can be applied is not from the peak pulse power, but from the noise that originates from the high power amplifier. The TWTA employed for this study (Applied Systems Engineering M/N 117) has a gated noise of approximately 1 mW that saturates the detection electronics, such that the detection of signal is not possible during the gated output of the TWTA. It is worth noting that the noise output of the solid-state amplifier (approximately 10 nW) pushes the detection electronics to near the saturation regime. However, with sufficient averaging the detector behaves linearly and we are able to detect signal. For the detector employed in the study a noise power of approximately 100 nW completely overwhelms the detection electronics and prevents detection of signal. Thus, with the current detection electronics and hardware, the use of the TWTA for the active

cancellation method is not feasible. This limitation may be overcome with new high power low noise solid-state amplifiers and low noise microwave sources, or a detector configuration that allows for a higher saturation point, which may be obtained by placing an attenuator in front of the microwave limiter.

The other issue is to overcome the non-linear nature of the TWTA, such that one could accurately control the shape and phase of the output waveform. The high power non-linear distortion of the TWTA on the shape and phase of an output waveform is reproducible. Therefore, in scenario lacking a physical model describing the transformation, one can calibrate for this via a lookup table or other empirical scheme, thus reliably controlling the output shape and phase of a given waveform.

Supplementary Material

Refer to Web version on PubMed Central for supplementary material.

Acknowledgements

We thank Steve Waltman (High Speed Circuit Consultants) for exceptional technical support and advice. We thank Dr. Daniel Sank, Dr. Yu Chen, Dr. Max Hofheinz, and Dr. Erik Lucero from the Martinis group for helpful advice pertaining to functioning of the FPGA and DAC boards of the AWG. We would also like to thank Brendan Allison, Bernhard Blümich, and Ilia Kaminker for helpful comments on the preparation of this manuscript. This work was funded by the NSF IDBR grant through the DBI division (1152244) and the NIH R21 grant on Instrument Development for Biomedical Applications (5R21GM103477-03).

REFERENCES

1. Borbat PP, Georgieva ER, Freed JH. Improved Sensitivity for Long-Distance Measurements in Biomolecules: Five-Pulse Double Electron-Electron Resonance. J. Phys. Chem. Lett. 2013; 4:170–175. doi:10.1021/jz301788n. [PubMed: 23301118]
2. Jeschke G. Distance measurements in the nanometer range by pulse EPR. Chemphyschem. 2002; 3:927–32. doi:10.1002/1439-7641(20021115)3:11<927::AID-CPHC927>3.0.CO;2-Q. [PubMed: 12503132]
3. Columbus L, Hubbell WL. A new spin on protein dynamics. Trends Biochem. Sci. 2002; 27:288–95. http://www.ncbi.nlm.nih.gov/pubmed/12069788. [PubMed: 12069788]
4. Gordon-Grossman M, Kaminker I, Gofman Y, Shai Y, Goldfarb D. W-Band pulse EPR distance measurements in peptides using Gd(3+)-dipicolinic acid derivatives as spin labels. Phys. Chem. Chem. Phys. 2011; 13:10771–80. doi:10.1039/c1cp00011j. [PubMed: 21552622]
5. Rizzatoa R, Bennati M. Enhanced sensitivity of electron-nuclear double resonance (ENDOR) by cross polarisation and relaxation. Phys. Chem. Chem. Phys. 2014; 16:7681–7685. doi:10.1039/c3cp55395g. [PubMed: 24647689]
6. Spindler PE, Glaser SJ, Skinner TE, Prisner TF. Broadband inversion PELDOR spectroscopy with partially adiabatic shaped pulses. Angew. Chem. Int. Ed. Engl. 2013; 52:3425–9. doi:10.1002/anie.201207777. [PubMed: 23424088]
7. Froncisz W, Camenisch TG, Ratke JJ, Anderson JR, Subczynski WK, Strangeway RA, et al. Saturation recovery EPR and ELDOR at W-band for spin labels. J. Magn. Reson. 2008; 193:297–304. doi:10.1016/j.jmr.2008.05.008. [PubMed: 18547848]
8. Robinson BH, Haas DA, Mailer C. Molecular dynamics in liquids: spin-lattice relaxation of nitroxide spin labels. Science. 1994; 263:490–3. http://www.ncbi.nlm.nih.gov/pubmed/8290958. [PubMed: 8290958]
9. Budil DE, Lee S, Saxena S, Freed JH. Nonlinear-Least-Squares Analysis of Slow-Motion EPR Spectra in One and Two Dimensions Using a Modified Levenberg–Marquardt Algorithm. J. Magn. Reson. Ser. A. 1996; 120:155–189. doi:10.1006/jmra.1996.0113.

10. Stoll S, Schweiger A. EasySpin, a comprehensive software package for spectral simulation and analysis in EPR. J. Magn. Reson. 2006; 178:42–55. doi:10.1016/j.jmr.2005.08.013. [PubMed: 16188474]
11. Schwartz LJ, Sillman AE, Freed JH. Analysis of electron spin echoes by spectral representation of the stochastic Liouville equation. J. Chem. Phys. 1982; 77:5410. doi:10.1063/1.443791.
12. Bonora M, Pornsuwan S, Saxena S. Nitroxide Spin - Relaxation over the Entire Motional Range. J. Phys. Chem. B. 2004:4196–4198.
13. Hoult DI. Fast recovery, high sensitivity NMR probe and preamplifier for low frequencies. Rev. Sci. Instrum. 1979; 50:193. doi:10.1063/1.1135786. [PubMed: 18699468]
14. Sullivan NS, Deschamps P, Neel P, Vaissiere JM. Efficient fast-recovery scheme for NMR pulse spectrometers. Rev. Phys. Appliquée. 1983; 18:253–261.
15. Lowe IJ, Barnaal DE. Radio-Frequency Bridge for Pulsed Nuclear Magnetic Resonance. Rev. Sci. Instrum. 1963; 34:143. doi:10.1063/1.1718288.
16. Alecci M, Placidi G, Testa L, Lurie DJ, Sotgiu A. Magnetic Resonance with Large Samples. J. Magn. Reson. 1998; 166:162–166.
17. Rinard GA, Quine RW, Ghim BT, Eaton SS, Eaton GR. Easily Tunable Crossed-Loop (Bimodal) EPR Resonator. J. Magn. Reson. Ser. A. 1996; 122:50–57. doi:10.1006/jmra.1996.0173.
18. Tsapin AI, Hyde JS, Froncisz W. Bimodal loop-gap resonator. J. Magn. Reson. 1992; 100:484–490. doi:10.1016/0022-2364(92)90055-C.
19. Rinard GA, Quine RW, Eaton GR. An L-band crossed-loop (Bimodal) EPR resonator. J. Magn. Reson. 2000; 144:85–8. doi:10.1006/jmre.2000.2014. [PubMed: 10783276]
20. Cruickshank PAS, Bolton DR, Robertson DA, Hunter RI, Wylde RJ, Smith GM. A kilowatt pulsed 94 GHz electron paramagnetic resonance spectrometer with high concentration sensitivity, high instantaneous bandwidth, and low dead time. Rev. Sci. Instrum. 2009; 80:103102. doi: 10.1063/1.3239402. [PubMed: 19895049]
21. Borneman TW, Cory DG. Bandwidth-limited control and ringdown suppression in high-Q resonators. J. Magn. Reson. 2012; 225:120–9. doi:10.1016/j.jmr.2012.10.011. [PubMed: 23165232]
22. Rudakov TN, Fedotov VV, Belyakov AV, Mikhal'tsevich VT. Suppression of transient processes in the oscillatory circuit of the NQR spectrometer. Instruments Exp. Tech. 2000; 43:78–81. doi: 10.1007/BF02759003.
23. Borbat PP, Crepeau RH, Freed JH. Multifrequency two-dimensional Fourier transform ESR: an X/Ku-band spectrometer. J. Magn. Reson. 1997; 127:155–67. [PubMed: 9281479]
24. Rinard GA, Quine RW, Eaton SS, Eaton GR, Froncisz W. Relative Benefits of Overcoupled Resonators vs Inherently Low-Q Resonators for Pulsed Magnetic Resonance. J. Magn. Reson. 1993; 108:71–81.
25. Davis JL, Mims WB. Use of a microwave delay line to reduce the dead time in electron spin echo envelope spectroscopy. Rev. Sci. Instrum. 1981; 52:131–132.
26. Narayana PA, Massoth RJ, Kevan L. Active microwave delay line for reducing the dead time in electron-spin echo spectrometry. Rev. Sci. Instrum. 1982; 53:624–626.
27. Kaufmann T, Keller TJ, Franck JM, Barnes RP, Glaser SJ, Martinis JM, et al. DAC-board based X-band EPR spectrometer with arbitrary waveform control. J. Magn. Reson. 2013; 235:95–108. [PubMed: 23999530]
28. Doll A, Pribitzer S, Tschaggelar R, Jeschke G. Adiabatic and fast passage ultra-wideband inversion in pulsed EPR. J. Magn. Reson. 2013; 230:27–39. doi:10.1016/j.jmr.2013.01.002. [PubMed: 23434533]
29. Doll A, Jeschke G. Fourier-transform electron spin resonance with bandwidth-compensated chirp pulses. J. Magn. Reson. 2014 doi:10.1016/j.jmr.2014.06.016.
30. Spindler PE, Zhang Y, Endeward B, Gershernzon N, Skinner TE, Glaser SJ, et al. Shaped optimal control pulses for increased excitation bandwidth in EPR. J. Magn. Reson. 2012; 218:49–58. doi: 10.1016/j.jmr.2012.02.013. [PubMed: 22578555]
31. Tseitlin M, Quine RW, a Rinard G, Eaton SS, Eaton GR. Digital EPR with an arbitrary waveform generator and direct detection at the carrier frequency. J. Magn. Reson. 2011; 213:119–25. doi: 10.1016/j.jmr.2011.09.024. [PubMed: 21968420]

32. Bialczak RC, Ansmann M, Hofheinz M, Lucero E, Neeley M, O'Connell A, et al. Quantum Process Tomography of a Universal Entangling Gate Implemented with Josephson Phase Qubits. Nat. Phys. 2009; 6:409–413. doi:10.1038/nphys1639.

33. Sun LI, Savory JJ, Warncke K. Design and Implementation of an FPGA-Based Timing Pulse Programmer for Pulsed-Electron Paramagnetic Resonance Applications. Concepts Magn. Reson. 2013; 43:100–109. doi:10.1002/cmr.b.

34. Maly T, Macmillan F, Zwicker K, Kashani-poor N, Brandt U, Prisner TF, et al. Relaxation Filtered Hyperfine (REFINE) Spectroscopy : A Novel Tool for Studying Overlapping Biological Electron Paramagnetic Resonance Signals Applied to Mitochondrial Complex I †. 2004:3969–3978.

35. Armstrong BD, Lingwood MD, McCarney ER, Brown ER, Blümler P, Han S. Portable X-band system for solution state dynamic nuclear polarization. J. Magn. Reson. 2008; 191:273–81. doi: 10.1016/j.jmr.2008.01.004. [PubMed: 18226943]

36. Twig Y, Dikarov E, Hutchison WD, Blank A. Note: High sensitivity pulsed electron spin resonance spectroscopy with induction detection. Rev. Sci. Instrum. 2011; 82:076105. doi: 10.1063/1.3611003. [PubMed: 21806239]

37. Blank A, Stavitski E, Levanon H, Gubaydullin F. Transparent miniature dielectric resonator for electron paramagnetic resonance experiments. Rev. Sci. Instrum. 2003; 74:2853–2859. doi: 10.1063/1.1568550.

38. Narkowicz R, Suter D, Niemeyer I. Scaling of sensitivity and efficiency in planar microresonators for electron spin resonance. Rev. Sci. Instrum. 2008; 79:1–8. doi:10.1063/1.2964926.

39. Narkowicz R, Suter D, Stonies R. Planar microresonators for EPR experiments. J. Magn. Reson. 2005; 175:275–284. doi:10.1016/j.jmr.2005.04.014. [PubMed: 15939642]

- We apply a high bandwidth AWG to completely remove the resonator ring down.
- We demonstrate the detection of EPR signal at any time during or after an excitation pulse.
- We demonstrate the complete recovery of a Hahn echo decay occurring during the ring down

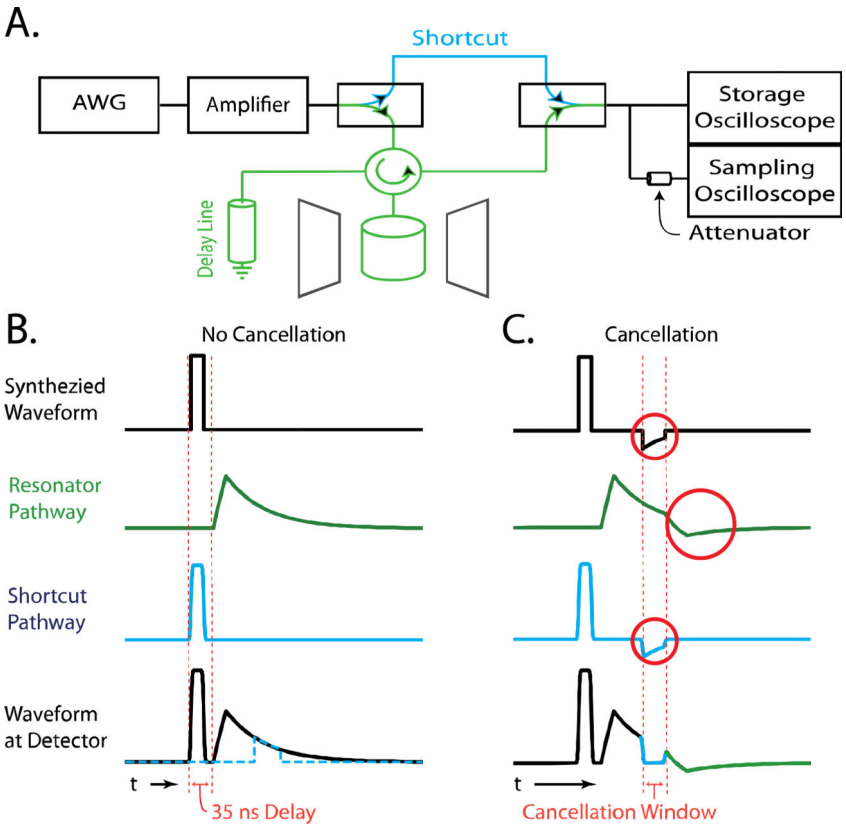

Figure 1.

The schematic of the delay line assembly is shown in A. The effect the delay line assembly has on a given excitation pulse is shown in B. A cancellation pulse is calculated from the ring-down shown in blue dashed line in B “waveform at detector”. The cancellation pulse, the negative of the blue dashed trace in B “waveform at detector”, is shown in the red circle behind the excitation pulse in C “synthesize waveform”. The cancellation pulse is shown circled in red in both the resonator and shortcut pathways of C. The cumulative effect of the cancellation pulse is shown in C “waveform at detector” where the respective colors correspond to the effect of the cancellation pulse from each individual pathway. The cancellation window is generated from the cancellation pulse, from the shortcut pathway, meeting with and destructively interfering with the ring-down, from the resonator pathway. Electron spin signal from the action of the excitation pulse alone is detectable inside of the 35 ns long cancellation window.

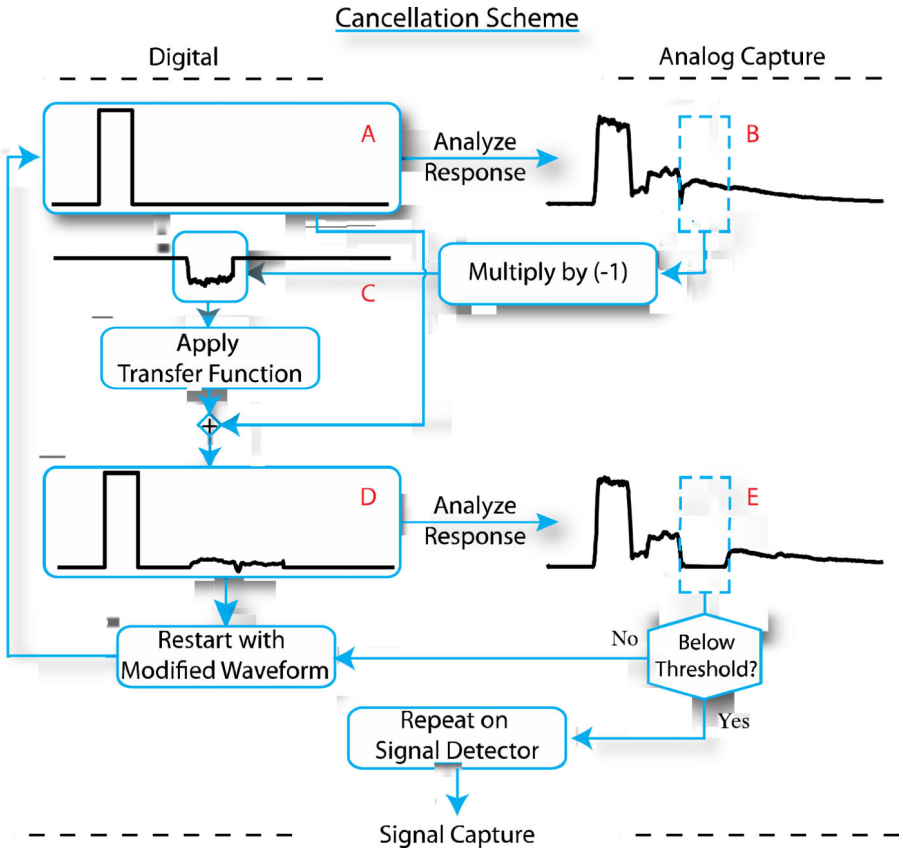

Figure 2.

The optimization scheme for producing and optimizing a given cancellation pulse. An initial digital excitation pulse (A) is synthesized, amplified, sent through the waveguide assembly, attenuated, and measured on a sampling oscilloscope (B). The transfer function for this specific cancellation pulse (shown as negative magnitude in C) is calculated and subsequently applied. The transfer function corrected cancellation pulse is spliced into the original digital excitation pulse at the correct relative time (D). Waveform (D) is synthesized and the residual microwave power remaining in the cancellation window is measured (E). If the residual power is above the threshold the cancellation pulse is optimized by restarting the scheme with waveform (D) in place of waveform (A) and the corrected cancellation pulse is added to the original cancellation pulse in waveform (A) instead of replacing the original cancellation pulse. Once the residual microwave power is below the threshold the higher sensitivity heterodyne signal detector is used to further optimize the cancellation pulse shape following the same scheme. Once the residual microwave power inside of the cancellation window is below 10 nW it is possible to observe EPR signal.

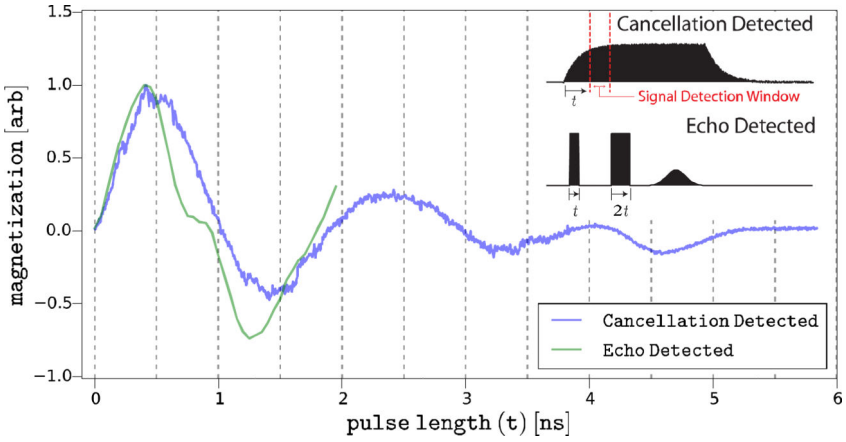

Figure 3.

The Rabi oscillation of the unpaired electron in the BDPA/PS sample measured with (blue) and without active cancellation (green). The inset illustrates the two separate schemes in which the Rabi oscillations are detected.

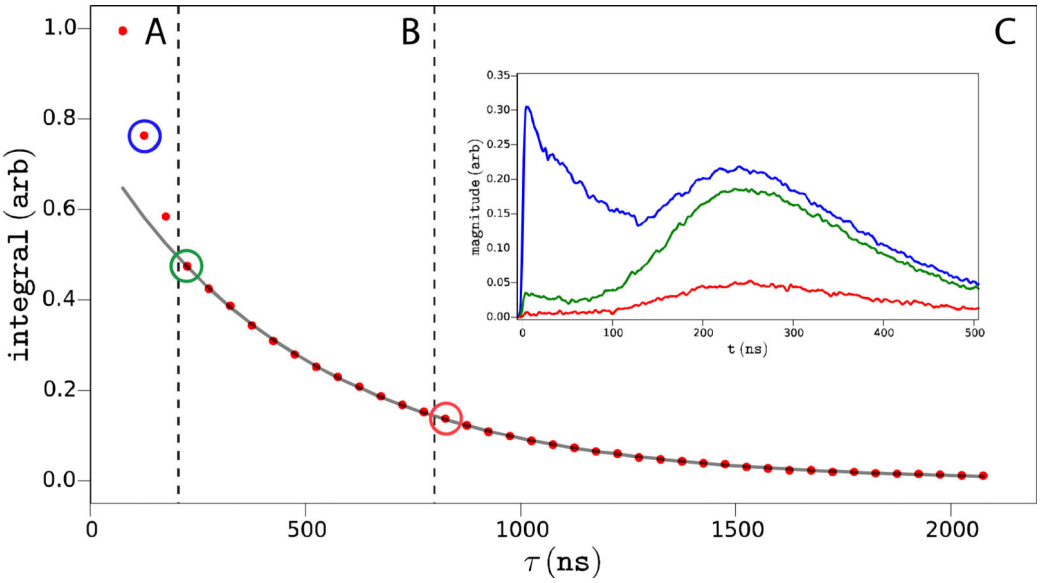

Figure 4.

The Hahn echo decay of the unpaired electron of BDPA embedded on a polystyrene matrix measured with a resonator Q of 800. The echoes corresponding to the colored circled data points are shown in the inset, where the time axis corresponds to the start of signal detection. Three regions are noted. In region C the echoes are detected after the ring-down has sufficiently decayed to allow for signal detection. In region B the echoes that are recovered during the detector dead-time by active cancellation. In region A the echoes are recovered by active cancellation but distorted by the 180° pulse.